Spred-2 deficiency exacerbates acetaminophen–induced hepatotoxicity in mice

Hiroshi Wakabayashi[a,b], Toshihiro Ito[a], Soichiro Fushimi[a], Yuki Nakashima[a], Jyunya Itakura[a], Liu Qiuying[a], Min Min Win[a], Sun Cuiming[a], Cao Chen[a], Miwa Sato[a], Ai Mino[a], Tetsuya Ogino[a], Hirofumi Makino[b], Akihiko Yoshimura[c], and Akihiro Matsukawa[a,*]

[a] *Department of Pathology and Experimental Medicine, Graduate School of Medical, Dentistry and Pharmaceutical Sciences, Okayama University, Okayama, Japan.*
[b] *Department of Medicine and Clinical Science, Graduate School of Medical, Dentistry and Pharmaceutical Sciences, Okayama University, Okayama, Japan.*
[c] *Department of Microbiology and Immunology, Keio University School of Medicine, Tokyo, Japan.*

[*]Correspondence author:

      Department of Pathology and Experimental Medicine,

      Graduate School of Medicine, Dentistry and Pharmaceutical Sciences,

      Okayama University, 2-5-1 Shikata, Okayama 700-8558, Japan.

      TEL&FAX: +81-86-235-7141

      E-mail: amatsu@md.okayama-u.ac.jp

Abbreviations:

      APAP: Acetaninophen, ALT: alanine transferase, ASGM1: asialo GM1,

      NAPQI: N-acetyl-p-benzoquinone imine, Spred: Sprouty-related

      EVH1-domain-containing protein

Abstract

MAPKs are involved in acetaminophen (APAP)-hepatotoxicity, but the regulatory mechanism remains unknown. Here, we explored the role of Spred-2 that negatively regulates Ras/ERK pathway in APAP-hepatotoxicity. Spred-2 knockout (KO) mice demonstrated exacerbated liver injury, an event that was associated with increased numbers of $CD4^+T$, $CD8^+T$ and NK cells in the liver compared to the control. Levels of CXCL9/CXCL10 that attracts and activates these cells were enhanced in Spred-2 KO-liver. Kupffer cells isolated from Spred-2 KO mice after APAP challenge expressed higher levels of CXCL9/CXCL10 than those from the control. Upon stimulation with APAP and IFNγ, naïve Kupffer cells from Spred-2 KO mice expressed higher levels of CXCL9/CXCL10. NK cell-depletion attenuated APAP-hepatotoxicity with lowered hepatic IFNγ and decreased numbers of not only NK cells but also $CD4^+T$ and $CD8^+T$ cells in the liver. These results suggest that Spred-2 negatively regulates APAP-hepatotoxicity under the control of Kupffer cells and NK cells.

1. Introduction

Acetaminophen (APAP) is widely used as a safety analgesic and antipyretic agent. Although considered safe at therapeutic doses, an accidental or intentional APAP overdose often causes acute liver failure with high morbidity and mortality [1]. The hepatotoxicity is mediated by a toxic metabolite N-acetyl-p-benzoquinone imine (NAPQI). Normally, NAPQI is detoxified by glutathione in the liver. In overdose glutathione is exhausted, thereby NAPQI covalently binds to cellular proteins and nonprotein thiols, initiating hepatocellular death due to oxidative stress. Hepatocyte injury in turn induces expressions of inflammatory molecules including cytokines and chemokines, resulting in an extensive severe liver damage [2].

There is a great interest in studying the cellular processes and signaling pathways during APAP-induced liver injury. We have found in a murine model of APAP-hepatotoxicity that suppressor of cytokine signaling (SOCS)3 in T cells negatively regulates hepato-damaging IFNγ☐signaling by inhibiting STAT1 activation[3]. IFNγ is also capable of activating MAPKs [4], another principal signaling pathway that includes JNK-1/2, p38 and ERK-1/2. MAPKs are activated by various extracellular stimuli such as oxidative stress, mitogens, hormones, growth factors, cytokines and chemokines [5]. As oxidative stress initiates APAP-hepatotoxicity [2], it is reasonable to speculate that MAPKs are involved in APAP-hepatotoxicity. In fact, mice injected with JNK inhibitor or lacking JNK (antisense treatment, siRNA, knock-out mice) were significantly protected against APAP-induced liver injury [6, 7], indicating a deleterious role of JNK-MAPK pathway. In contrast, p38-MAPK pathway does not appear to play a role [8]. ERK is also activated by APAP [7], but the contribution of ERK-MAPK pathway in APAP-hepatotoxicity remains unclear.

Dysregulation of MAPKs may cause exacerbation of APAP-hepatotoxicity. Sprouty-related EVH1-domain-containing protein (Spred) is a family of proteins that

inhibit Ras-dependent ERK signaling. Spred-2 is ubiquitously expressed in various tissues including liver whereas Spred-1 and Spred-3 are preferentially expressed in the brain and cerebellum [9, 10]. However, the physiological functions of Spred proteins in the liver pathology remain largely unknown. In the present study, we have focused on Spred-2 and investigated the role in the evolution of APAP-induced liver injury. We demonstrate that Spred-2 knockout (KO) mice show enhanced APAP-hepatotoxicity. Our results suggest that the exacerbated liver injury in Spred-2 KO mice is due to the increased numbers of hepatotoxic lymphocytes such as $CD4^+T$ cells, $CD8^+T$ cells and NK cells, possibly by augmented CXCL9 and CXCL10 under the control of Kupffer cells and NK cells.

2. Materials and Methods

2.1. Mice

Spred-2 KO mice backcrossed into the C57BL/6J background have been previously reported [11, 12]. C57BL/6J mice were used as the wild-type (WT) mice. These mice were transferred to the Department of Animal Resources, Okayama University (Okayama, Japan) and then bred at the facility. Female mice (6-8 weeks) were used in this study under specific pathogen-free conditions. The mice were housed in a temperature-controlled environment with a 12-hour light/12-hour dark cycle and allowed free access to water and food. The animal care and use committee at Okayama University approved all experiments conducted in this study.

2.2. APAP-induced liver injury

Fresh suspensions of APAP (Sigma Chemical Co., St. Louis, MO) were made immediately before use by dissolving the compound in phosphate-buffered saline (PBS) warmed to 40°C [3]. Mice were fasted for 12 h with free access to water and then

4

received intraperitoneal (i.p.) injection of APAP (400 mg/kg). At appropriate time intervals after APAP injection, mice were anesthetized, bled and sacrificed. Serum levels of alanine aminotransferase (ALT) were measured using standardized techniques. The livers were perfused with saline, excised, snap frozen in liquid nitrogen, and stored at -80°C for subsequent analyses. A part of the liver was fixed in 10% formalin, embedded in paraffin, and the liver sections were stained with hematoxylin and eosin. For some experiments, NK cells and Kupffer cells were deleted prior to APAP challenge. For NK cell-deletion, reconstituted anti-asialo GM1 antiserum (ASGM1; 20 μl/mouse, Wako Pure Chemical Industries, Osaka, Japan) was i.p. injected 12 h prior to APAP challenge [13]. Normal rabbit serum was used as a control. To delete Kupffer cells, mice were i.v. injected with 200 μl of clodronate encapsulated liposomes (Encapsula Nanosciences, Nashville, TN) 1 and 2 days before APAP-challenge. Empty liposomes were used as a control. All mice experiments were repeated two to three times and confirmed the reproducibility.

2.3. Detection of apoptosis and caspase activity

DNA fragmentation is a key feature of apoptosis. To detect DNA fragmentation in paraffin-embedded liver sections, ApopTag In Situ Detection Kit (Chemicon International, Inc., Temecula, CA) was used, according to manufacturers' instructions. For the measurement of caspase-3, -8, -9 activities, colorimetric assay kit (MBL, Nagoya, Japan) for each caspase was used. The livers were homogenized in lysis buffer provided by the kit and the activities in the cytosolic extracts (100 μg protein) were measured with a kit. Protein concentrations in the extracts were measured by protein-dye binding assay (Bio-Rad Laboratories, Hercules, CA).

2.4. Reverse transcription-PCR (RT-PCR)

The tissues were homogenized in Trizol Reagent (Gibco BRL, Grand Island, NY), and

total RNA was isolated. First-strand cDNA was constructed from 2 μg of total RNA with oligo $(dT)_{12-18}$ as primers, and the cDNAs were used as a template for PCR. Quantitative real-time PCR for Fas and FasL was performed with a StepOne with Power SYBR PCR master mix (Applied Biosystems, Foster City, CA). The primers were as follows: Fas, sense: 5'-CTGCGATGAAGAGCATGGTTT-3'; anti-sense: 5'-CCATAGGCGATTTCTGGGAC-3'. FasL, sense: 5'-AAGAAGGACCACAACACAAATCTG-3'; anti-sense: 5'-CCCTGTTAAATGGGCCACAC-3'. To validate the SYBR Green PCR products, a dissociation step was done to verify the T_m (annealing temperature) of the SYBR Green PCR product after the PCR were run. The expression levels of each mRNA were normalized by the expression of a housekeeping gene β-actin (sense: 5'-GGTCATCACTATTGGCAACG-3'; anti-sense: 5'-ACGGATGTCAACGTCACACT-3'). mRNA expressions for IFNγ, CXCL9, CXCL10, CXCR3 and Spred-2 were measured by Taqman RT-PCR using GAPDH as the internal standard (Applied Biosystems). A standard Gel electrophoresis/RT-PCR was also carried out for Spred-2 and GAPDH. The primers were as follows: Spred-2, sense: 5'-TGTGAGCACCGGAAGATTTATACC-3'; anti-sense: 5'-CGCGGCGGCTTTGTGCTT-3'. GAPDH, sense: 5'-TGTTCCAGTATGACTCCACTCACG-3'; anti-sense: 5'-TCTGGGTGGCAGTGATGGCATGGA-3'. The PCR was carried out at 95°C 3 min, 26 cycles of 95°C for 10 sec, 55°C for 10 sec, and 74°C for 1 min, and 74°C for 5 min. Ten microliters of PCR products were subjected to electrophoresis on a 2% agarose gel in presence of ethidium bromide, photographed and digitized.

2.5. Isolation of hepatic leukocytes

Hepatic leukocytes were isolated from the fresh liver [14]. In brief, mice were anesthetized and the livers were perfused in situ via the portal vein with 60 ml of HBSS at

a flow rate of 5 ml/min and then removed. The livers were minced and digested with 0.02% (w/v) collagenase and 0.0005% (w/v) DNase I in HBSS containing 20 mM HEPES, pH 7.4, at 37 °C for 30 min with occasional shaking. The resulting cell suspension was filtered through a 75-μm nylon mesh and the filtrate was washed once with HBSS, layered over a 1.037 g/ml solution of Percoll (GE healthcare Bio-Sciences, Uppsala, Sweden) and centrifuged at $400 \times g$ for 20 min. The resulting upper layer and interface, containing Ito cells, dead cells, and debris, were removed. The lower layer was diluted with Dulbecco's PBS and centrifuged at $600 \times g$ for 10 min to pellet the cells, re-suspended with PBS and the total cell numbers were counted by hemocytometer.

2.6. Flow cytometry

Hepatic leukocytes were suspended in PBS supplemented with 2% FCS and 0.1% sodium azaide, and stained with fluorescein isothiocyanate (FITC)-conjugated anti-CD3 (145-2C11), phycoerythrin (PE)-conjugated anti-CD4 (GK1.5), FITC-conjugated anti-CD8 (53-6.7), FITC-conjugated anti-CD25 (3C7), PE-conjugated anti-NK1.1 (PK136), FITC-conjugated Ly6G (RB6-8C5)(BD Pharmingen, San Jose, CA), PerCP/Cy5.5-conjugated CD11b (M1/70), PE-conjugated F4/80, FITC-conjugated IFNγ (BioLegend, San Diego, CA), PE-conjugated granzyme B and PE-conjugated perforin (eBioscience, San Diego, CA). The number of leukocyte populations in each liver was calculated by multiplying the respective percentages, as determined via flow cytometry, by total hepatic leukocyte counts. In case of intracellular staining for IFNγ, perforin and granzyme B, fixation/permealization and permealization buffers were used (eBioscience). The positive cell numbers was determined by gating on the respective cell types. Stained cells were analyzed using a Cell Lab Quanta SC MPL (Beckman Coulter, Inc., Brea, CA).

2.7. Splenocytes culture

Spleens were excised from WT and Spred-2 KO mice at 12 h after APAP treatment, and

the splenocytes were dispersed into single-cell suspensions. After lysing red blood cells, the cells (5×10^6 cells/ml) were suspended in RPMI 1640 supplemented with 5% FCS, glutamine and antibiotics and cultured for 72 h without stimulation. The culture supernatants were used for measurement of cytokines.

2.8. Kupffer cell isolation and culture

Non-parenchymal cells were isolated as described above. CD11b$^+$ cells were isolated from the cells by anti-CD11b microbeads over MS$^+$ MiniMACS separation columns (Miltenyi Biotec, Bergisch-Gladbach, Germany) according to instructions supplied by the manufacturer. Most of the purified cells were alive (>97%, trypan blue exclusion) and routinely >95% CD11b$^+$ cells. The cells were plated onto 24 well at a density of 3×10^5 cells per well, incubated for 1 h, non-adherent cells were washed off with RPMI1640 and fresh medium containing 10% FBS, glutamine and antibiotics was added. The adherent Kupffer cells were then stimulated with APAP (10 μg/ml) and IFNγ (10 ng/ml) for 4 h. RNA from each sample was purified using High Pure RNA Isolation Kit (Roche Diagnostics, Mannheim, Germany).

2.9. Western blotting

Cleared supernatants of liver homogenates were boiled with sample buffer that contained 1% SDS, 10 mmol/L Tris-HCl (pH 7.5), fractionated on SDS-polyacrylamide gel, and transferred to a nitrocellulose membrane. After blocking with TBS-T (Tris-buffered saline + 0.1% Tween-20) containing 5% skim milk for 1 h at room temperature, the membrane was incubated with antibodies to p44/42 MAPK (Erk1/2), phospho-p44/42 MAPK (Erk1/2), SAPK/JNK, phospho-SAPK/JNK, p38 MAPK, and phospho-p38 MAPK (Cell Signaling Inc, Beverly, MA) overnight at 4°C. After washing with TBS-T, the membrane was incubated with anti-HRP-linked antibody for 1 h at room temperature and visualized with an enhanced chemiluminescence system (Cell Signaling),

photographed and digitized.

2.10. Measurement of cytokines

Murine cytokines were measured using a standard method of sandwich ELISA, as described [15, 16]. The captured antibodies, detection antibodies and the recombinant cytokines were purchased from R&D Systems (Minneapolis, MN). The ELISAs employed in this study did not cross-react with other murine cytokines available. For cytokine measurement in the liver, livers were homogenized in PBS containing 0.1% TritonX-100 and complete protease inhibitor (Roche), centrifuged, and the cleared supernatants were obtained.

2.11. Statistics

Statistical significance was evaluated by ANOVA. A $p < 0.05$ was regarded as statistically significant. All data were expressed as mean ± SEM.

3. Results

3.1. Expression and role of Spred-2 in APAP-induced liver injury

To investigate the role of Spred-2, first experiments were conducted to examine the expression of endogenous Spred-2 in the liver. Consistent with previous reports [10, 17], Spred-2 was constitutively expressed in the liver. The expression level was increased and peaked at 3 h after APAP challenge (Fig. 1A), suggesting that endogenous Spred-2 might be involved in APAP-induced liver injury.

To understand the contribution of Spred-2 in APAP-hepatotoxicity, we employed Spred-2 KO mice. No appreciable level of Spred-2 was detected in Spred-2 KO-liver (Fig. 1A inset). Taqman RT-PCR also showed no Spred-2 expression in Spred-2 KO-liver (data not shown). The data in Figure 1B demonstrated that ALT level, a

specific marker of liver injury, was significantly increased in Spred-2 KO mice as compared to WT controls. Histologically, centrilobular liver necrosis was much severer in Spred-2 KO mice than that in the WT mice (Fig. 1C and D). There was no significant difference in basal level of ALT between the groups (WT vs. Spred-2 KO, 64.9 ± 7.4 vs. 65.7 ± 9.7 IU/L, not significant, 5 mice each). Basal glutathione levels in the liver were similar between the groups (WT vs. Spred-2 KO, 1.7 ± 0.1 vs. 1.9 ± 0.1 mM/g liver, not significant, 5 mice each). Thus, Spred-2 KO mice demonstrated exacerbated liver injury after APAP challenge.

3.2. Hepatocyte apoptosis in Spred-2 KO mice

In the mechanistic level, we first asked whether APAP-induced hepatocyte apoptosis would be augmented in Spred-2 KO mice. TUNEL staining of liver sections at 6 h post-APAP showed that apoptotic hepatocytes were increased in Spred-2 KO-liver, relative to the control (Fig. 2A and B). Caspases are a class of cysteine proteases involved in apoptosis. The data in Figure 2C demonstrated that activities of caspase-3, -8 and -9 in WT-liver were comparatively increased after APAP challenge, which were slightly augmented in Spred-2 KO-liver. Apoptosis is often initiated by death ligand/death receptor interactions, such as Fas ligand (FasL) with Fas, leading to a caspase activation cascade. mRNA expression of FasL, but not Fas, at 6 h post APAP was relatively increased in Spred-2 KO-liver compared to the controls (Fig. 2D). Thus, the increases in caspases/FasL in Spred-2 KO-liver were modest, suggesting that these pathways were unlikely the main cause of augmented liver injury in Spred-2 KO mice.

3.3. Leukocyte populations in the liver after APAP challenge

Liver histology in APAP-induced liver injury in humans shows hepatocyte damage with lymphocytic accumulation [18]. Experiments were conducted to examine the leukocyte populations in the liver. As shown in Figure 3A, the numbers of total leukocytes in the

liver were increased with time in WT mice, which was significantly augmented in Spred-2 KO mice. FACS analyses at 6 h post APAP challenge revealed that hepatotoxic lymphocytes that include CD4$^+$T cells, CD8$^+$T cells and NK cells (CD3$^-$NK1.1$^+$) were significantly increased in Spred-2 KO-liver as compared to the control (Fig. 3B). No difference was found in the numbers of NKT cells (CD3$^+$NK1.1$^+$), macrophages (CD11b$^+$F4/80$^+$), neutrophils (CD11b$^+$Ly6G$^+$) and regulatory T cells (CD4$^+$CD25$^+$) between WT- and Spred-2 KO-liver (WT vs. Spred-2 KO: 2.1 ± 0.2 vs. 2.4 ± 3.4, 0.5 ± 0.2 vs. 5.9 ± 0.2, 2.1 ± 0.6 vs. 2.8 ± 0.5, 0.4 ± 0.1 vs. 0.8 ± 0.2, $\times 10^5$ cells/liver, not significant, 14 mice each). There were no significant differences in the basal numbers of leukocyte populations between the groups (WT vs. Spred-2 KO: CD4$^+$ T; 10.6 ± 1.4 vs. 11.1 ± 2.3, CD8$^+$ T; 5.0 ± 0.9 vs. 4.9 ± 0.8, NK; 3.9 ± 0.9 vs. 3.9 ± 1.0, NKT; 12.5 ± 2.2 vs. 10.1 ± 2.2, macrophage; 4.5 ± 1.3 vs. 6.1 ± 1.3, neutrophils; 3.9 ± 0.4 vs. 2.8 ± 0.3, $\times 10^4$ cells/liver, not significant, 4 mice each). Thus, APAP-induced leukocyte populations such as CD4$^+$T cells, CD8$^+$T cells and NK cells in the liver were augmented in Spred-2 KO mice.

3.4. Increased IFNγ, CXCL9 and CXCL10 in Spred-2 KO mice

APAP overdose results in elevated cytokines in the circulation. IFNγ is crucial in APAP-hepatotoxicity [19, 20], which stimulates the production of IFNγ-inducible chemokine CXCL9/CXCL10 that attracts and activates hepatotoxic lymphocytes such as CD4$^+$T cells, CD8$^+$T cells and NK cells [21]. We therefore investigated the cytokine response after APAP challenge. The data in Figure 4A showed that circulating levels of IFNγ, CXCL9 and CXCL10 were elevated in Spred-2 KO mice in comparison to those in WT mice. Hepatic levels of CXCL9, CXCL10 and their receptor CXCR3 were increased in Spred-2 KO mice (Fig. 4B). Basal levels of these cytokine/chemokines were negligible in WT and Spred-2 KO liver (data not shown). Although IFNγ level in whole livers were unchanged between the groups, the numbers of IFNγ positive-CD4$^+$T cells, CD8$^+$T cells and NK cells in Spred-2 KO mice were significantly augmented as

compared to the WT mice (Fig. 4C). The number of IFNγ positive cells in NKT cells remained unchanged between WT and Spred-2 KO mice (data not shown). Basal levels of IFNγ positive cells were very low and equivalent between the groups (WT vs. Spred-2 KO: CD4$^+$T; 0.22 ± 0.09 vs. 0.55 ± 0.42, CD8$^+$T; 0.02 ± 0.02 vs. 0.05 ± 0.05, NK; 0.41 ± 0.05 vs. 0.98 ± 0.57, NKT; 2.79 ± 0.89 vs. 1.12 ± 0.91, $\times 10^3$ cells/liver, not significant, 3 mice each). Given the early expression pattern of Spred-2 in the liver (Fig. 1A), Spred-2 might alter cytokine response by affecting the other MAPK pathways. The data in Figure 4D demonstrated that not only ERK- but also JNK- and p38-activation was enhanced in Spred-2 KO-liver relative to the control. Thus, deletion of Spred-2 demonstrated elevated hepatotoxic cytokine/chemokine response with boosted activation of multiple MAPK pathways.

3.5. Cells responsible for enhanced IFNγ, CXCL9 and CXCL10 in Spred-2 KO mice

Splenocytes harvested from either APAP-treated WT or Spred-2 KO mice did not spontaneously release appreciable levels of IFNγ, CXCL9 and CXCL10 (data not shown), suggesting that these cytokine/chemokines were produced not from circulating cells rather from cells in the liver. Kupffer cells are resident macrophage population in the liver with a potent capacity to produce multiple cytokines/chemokines [22], suggesting a possible source of hepatotoxic cytokine/chemokines in this model. To address this, Kupffer cells were isolated from WT and Spred-2 KO mice after APAP challenge and the expressions of these cytokine/chemokines were measured. As shown in Figure 5A, expressions of CXCL9 and CXCL10 in Kupffer cells were significantly elevated in Spred-2 KO mice as compared to those in WT mice. IFNγ was not detected in Kupffer cells from WT and Spred-2 KO mice (not shown). Accordingly, Kupffer cells were isolated from non-treated WT and Spred-2 KO mice and stimulated with APAP *in vitro*, which demonstrated that Kupffer cells from Spred-2 KO mice expressed significantly

higher levels of CXCL9 and CXCL10 than those from the WT mice (Fig. 5B). No IFNγ was detected from WT- and Spred-2 KO-Kupffer cells (data not shown). Upon stimulation with IFNγ, naïve Kupffer cells from Spred-2 KO mice also expressed higher levels of CXCL9 and CXCL10 in comparison to the controls (Fig. 5C) with no endogenous IFNγ (data not shown). The results suggest that Kupffer cells could be the source of the augmented CXCL9 and CXCL10 in Spred-2 KO mice. Together with data in Figure 4C, IFNγ appears to be derived from hepatotoxic lymphocytes.

3.6. NK cells affect the augmented hepatotoxic T cell response in Spred-2 KO mice

NK cells are known play a central role in APAP-hepatotoxicity by producing IFNγ [20]. To understand the role of NK cells in this model, we attempted to delete NK cells by anti-ASGM1 in Spred-2 KO mice. The data in Figure 6A showed that anti-ASGM1 treatment significantly decreased IFNγ expression in the liver. Under the conditions, ALT level was decreased for up to 50% after the treatment with anti-ASGM1 (Fig. 6B). Histologically, centrilobular liver necrosis induced by APAP was dramatically improved by anti-ASGM1 as compared to the control (Fig. 6C). FACS analyses revealed that expression of perforin and granzyme B, injurious molecules produced from NK cells and CD8$^+$ T cells, was reduced in Spred-2 KO-liver (Fig. 6D).

Leukocyte populations after anti-ASGM1 treatment were next examined. Anti-ASGM1 treatment resulted in an 87% reduction in the number of NK cells in the liver (Table 1). Subsequently, other leukocyte populations were also examined in the liver. Hepatic number of NKT cells was not affected by anti-ASGM1. Very interestingly, the numbers of CD4$^+$T cells and CD8$^+$T cells in the liver were considerably decreased after anti-ASGM1 treatment. Conversely, there was a trend toward increase in the number of CD4$^+$FoxP3$^+$T cells (p=0.14). The number of macrophages (CD11b$^+$F4/80$^+$ cells) was unchanged while that of neutrophils (CD11b$^+$Ly6G$^+$ cells) was decreased by 50% although it was not statistically significant (Table 1). IFNγ positive cells in CD8$^+$T

and NKT cells, but not CD4$^+$T cell were decreased in mice treated with anti-ASGM1 (Fig. 6E). Thus, depletion of NK cells attenuated APAP-hepatotoxicity in Spred-2 KO mice, an event that was associated with decreased numbers of CD4$^+$T and CD8$^+$T cells and decreased IFNγ positive cells in CD8$^+$T cells and NKT cells. NK cells appear to be crucial in the subsequent recruitment of leukocytes and production of IFNγ from specific cell populations.

4. Discussion

Molecular interactions between toxicants and biological pathways are an emerging field of toxicology. Ras is a key-signaling molecule, and Spred proteins have a negative impact on Ras/Raf/ERK pathway by binding to Ras and consequently inhibiting phosphorylation of Raf [17]. In the present study, we have focused on Spred-2 in liver immunology and demonstrated for the first time that Spred-2 is protective in APAP-induced hepatotoxicity, as deletion of Spred-2 was vulnerable to the injury.

The exaggerated liver injury in Spred-2 KO mice appeared to be ascribed to the augmented numbers of hepatotoxic lymphocytes such as CD4$^+$T cells, CD8$^+$T cells and NK cells. IFNγ is crucial in the immune response during APAP-hepatotoxicity [19, 20]. Both CD4$^+$ cells and CD8$^+$T cells, known as type I effector T cells, are major sources of IFNγ. NK cells are deleterious in APAP-hepatotoxicity by producing IFNγ [20]. In this study, we showed that IFNγ-positive CD4$^+$T cells, CD8$^+$T cells and NK cells were increased in the liver from Spred-2 KO mice. In addition, IFNγ-inducible CXCL9/CXCL10 that attracts and activates these cell types was significantly augmented in the liver form Spred-2 KO mice. Increased CXCL9 and CXCL10 in Spred-2 KO mice appeared to result from the activation of Ras and p38. Activation of Ras promoted the overexpression of CXCL10 in human breast cancer cells primarily through the Raf and PI3K signaling pathways [23]. p38 participated in the regulation of CXCL9/CXCL10 expression [4]. The numbers of NKT cells; also known to be deleterious in

14

APAP-hepatotoxicity were unchanged in our model, although the cells can be attracted by CXCL9 and CXCL10. This may be a result of activation-induced cell death or loss of surface marker expression of NKT cells [24, 25].

Very interestingly, reduction of NK cells with anti-ASGM1 significantly decreased APAP-induced liver injury with reduction in the hepatic numbers of not only NK cells but also CD4$^+$T cells and CD8$^+$T cells. Liver lymphocytes are abundant in NK cells (5-10%) and play an important role in first-line innate defense in the liver. NK cells directly and indirectly kill target cells by enhancing immune response through IFNγ production [26]. Decreased CD4$^+$T cells and CD8$^+$T cells by anti-ASGM1 may be its direct effect on these cells. It has demonstrated that ASGM1 is also expressed on certain CD4$^+$T cells [27] and CD8$^+$T cells [28]. Alternatively, NK cell deletion by anti-ASGM1 may affect regulatory T cell differentiation. Activated NK cells interfere with CD28-mediated Foxp3 expression in CD4$^+$CD25$^-$T cells [29]. NK cells lyse CD4$^+$CD25$^+$Foxp3$^+$T cells in certain conditions [30]. In the present study, NK cell depletion led to a trend toward increase in the number of regulatory T cells. The mechanism underlying the effects of anti-ASGM1 deserves attention. Employing anti-NK1.1 antibody or NKT-KO mice (CD1dKO mice) could be helpful to further understand the mechanism(s).

A previous study suggested that NK and NKT cells were not involved in APAP-hepatotoxicity [31]. Unlike in case of dimethylsulfoxide (DMSO) as a solvent, APAP failed to activate and recruit hepatic NK and NKT cells when dissolved in saline, suggesting that DMSO may play a role. However, in the present study, we clearly showed that APAP dissolved in PBS actually activated hepatic NK cells but not NKT cells as evidenced by increased NK cell numbers and higher intracellular levels of IFNγ, which was augmented in Spred-2 KO mice. We believe that NK cells play a role in APAP-hepatotoxicity under physiological conditions.

Kupffer cells are located within the lumen of the liver sinusoids, and are the

first cell population encounters various stimuli including toxins, and release reactive oxygen species (ROS), cytokines and chemokines upon stimulation [22]. Our results suggest that Kupffer cells are responsible for the augmented CXCL9 and CXCL10 response in Spred-2 KO mice. NK cells together with Kupffer cells are preferentially located in the hepatic sinusoids, often adhering to the endothelial cells [32]. NK cells may assist Kupffer cells to induce CXCL9 and CXC10 by releasing IFNγ.

A question arises whether deletion of Kupffer cells could dampen the augmented liver injury in Spred-2 KO mice. The functional role of Kupffer cells in APAP-hepatotoxicity remains controversial. Previous studies showed that APAP-hepatotoxicity could be dramatically reduced by several Kupffer cell inactivators [33]; however, others showed an exacerbated APAP-liver injury in the absence of Kupffer cells [34, 35]. After Kupffer cell deletion with liposome/clodronate, we failed to reduce the augmented APAP-hepatotoxicity in Spred-2 KO mice. Serum ALT level was rather increased (liposome/control vs. liposome/clodronate, $5{,}152 \pm 2{,}461$ IU/L vs. $10{,}200 \pm 3{,}464$ IU/L, $p=0.35$, 5 each), where liposome/clodronate decreased 70-80% of $CD11b^+F4/80^+$ cells at time 0 and 12 h after APAP challenge. Consistent with a previous report [35], Kupffer cell depletion by liposome/clodronate led to decreases in the hepatic level of hepato-regulatory cytokine IL-10 although it was not statistically significant (Relative expression: liposome/control vs. liposome/clodronate, 2.6 ± 1.7 vs. 0.06 ± 0.03, $p=0.167$, 5 each), suggesting that Kupffer cells or infiltrating macrophages are a significant source of IL-10. Recently, it has demonstrated that M2 macrophages that generate IL-10 are recruited into the liver after APAP challenge [36]. Mice deficient in CC chemokine receptor 2 (CCR2), the receptor for CCL2, showed reduced M2 accumulation during APAP hepatotoxicity and consequently a substantial delay in tissue repair with increased neutrophil infiltration [36, 37]. These data suggest that liposome/clodronate also deletes M2 macrophage from the body, resulting in an enhanced APAP-induced liver injury via decreased IL-10. Thus, the controversy may

stem from the heterogeneity and/or plasticity of macrophages and the difficulty in distinguishing and differentially studying subpopulations of macrophages in the liver.

The other point needs to address in this study is the role of Spred-2 in parenchymal hepatocytes. Lacking Spred-2 in hepatocytes may directly affect APAP-hepatotoxicity. Hepatocytes are known to produce CXCL9 and CXCL10 [38]. However, using primary hepatocytes from WT and Spred-2 KO-liver, we did not find altered hepatocyte damage (LDH release from the cells) and CXCL9/CXCL10 expression after stimulation with APAP and NAPQI (not shown). It remains undetermined whether inhibition of ERK or JNK in hepatocytes could inhibit lymphocyte infiltration and IFNγ/chemokine production in these mice. The function of Spred-2 in parenchymal hepatocytes needs to be further investigated.

APAP poisoning accounts for approximately one-half of all cases of acute liver failure in the United States and Great Britain. A better understanding of the signaling pathways involved in animal model may lead to novel insights and possible therapeutic targets. In the present study, we have shown that lacking Spred-2 is deleterious in APAP-induced liver injury by enhancing hepatotoxic lymphocyte response, suggesting that Spred-2 may be a therapeutic target for the treatment of APAP-induced hepatotoxicity.

Acknowledgments

References

[1]   N. Kaplowitz, Idiosyncratic drug hepatotoxicity, Nat. Rev. Drug Discov. 4 (2005) 489-499.

[2]   Z.X. Liu, N. Kaplowitz, Role of innate immunity in acetaminophen-induced hepatotoxicity, Expert Opin. Drug Metab. Toxicol. 2 (2006) 493-503.

[3]   K. Numata, M. Kubo, H. Watanabe, K. Takagi, H. Mizuta, S. Okada, S.L. Kunkel, T. Ito, A. Matsukawa, Overexpression of suppressor of cytokine signaling-3 in T cells exacerbates acetaminophen-induced hepatotoxicity, J. Immunol. 178 (2007) 3777-3785.

[4]   A.F. Valledor, E. Sanchez-Tillo, L. Arpa, J.M. Park, C. Caelles, J. Lloberas, A. Celada, Selective roles of MAPKs during the macrophage response to IFN-gamma, J. Immunol. 180 (2008) 4523-4529.

[5]   E.K. Kim, E.J. Choi, Pathological roles of MAPK signaling pathways in human diseases, Biochim. Biophys. Acta 1802 (2010) 396-405.

[6]   B.K. Gunawan, Z.X. Liu, D. Han, N. Hanawa, W.A. Gaarde, N. Kaplowitz, c-Jun N-terminal kinase plays a major role in murine acetaminophen hepatotoxicity, Gastroenterology 131 (2006) 165-178.

[7]   B.D. Stamper, T.K. Bammler, R.P. Beyer, F.M. Farin, S.D. Nelson, Differential regulation of mitogen-activated protein kinase pathways by acetaminophen and its nonhepatotoxic regioisomer 3'-hydroxyacetanilide in TAMH cells, Toxicol. Sci. 116 (2010) 164-173.

[8]   H. Nakagawa, S. Maeda, Y. Hikiba, T. Ohmae, W. Shibata, A. Yanai, K. Sakamoto, K. Ogura, T. Noguchi, M. Karin, H. Ichijo, M. Omata, Deletion of apoptosis signal-regulating kinase 1 attenuates acetaminophen-induced liver injury by inhibiting c-Jun N-terminal kinase activation, Gastroenterology 135 (2008) 1311-1321.

[9]   C.M. Engelhardt, K. Bundschu, M. Messerschmitt, T. Renne, U. Walter, M.

Reinhard, K. Schuh, Expression and subcellular localization of Spred proteins in mouse and human tissues, Histochem. Cell Biol. 122 (2004) 527-538.

[10] R. Kato, A. Nonami, T. Taketomi, T. Wakioka, A. Kuroiwa, Y. Matsuda, A. Yoshimura, Molecular cloning of mammalian Spred-3 which suppresses tyrosine kinase-mediated Erk activation, Biochem. Biophys. Res. Commun. 302 (2003) 767-772.

[11] I. Nobuhisa, R. Kato, H. Inoue, M. Takizawa, K. Okita, A. Yoshimura, T. Taga, Spred-2 suppresses aorta-gonad-mesonephros hematopoiesis by inhibiting MAP kinase activation, J. Exp. Med. 199 (2004) 737-742.

[12] K. Taniguchi, R. Kohno, T. Ayada, R. Kato, K. Ichiyama, T. Morisada, Y. Oike, Y. Yonemitsu, Y. Maehara, A. Yoshimura, Spreds are essential for embryonic lymphangiogenesis by regulating vascular endothelial growth factor receptor 3 signaling, Mol. Cell Biol. 27 (2007) 4541-4550.

[13] M. Kasai, M. Iwamori, Y. Nagai, K. Okumura, T. Tada, A glycolipid on the surface of mouse natural killer cells, Eur. J. Immunol. 10 (1980) 175-180.

[14] H. Do, J.F. Healey, E.K. Waller, P. Lollar, Expression of factor VIII by murine liver sinusoidal endothelial cells, J. Biol. Chem. 274 (1999) 19587-19592.

[15] A. Matsukawa, M.H. Kaplan, C.M. Hogaboam, N.W. Lukacs, S.L. Kunkel, Pivotal role of signal transducer and activator of transcription (Stat)4 and Stat6 in the innate immune response during sepsis, J. Exp. Med. 193 (2001) 679-688.

[16] A. Matsukawa, S. Kudo, T. Maeda, K. Numata, H. Watanabe, K. Takeda, S. Akira, T. Ito, Stat3 in resident macrophages as a repressor protein of inflammatory response, J. Immunol. 175 (2005) 3354-3359.

[17] T. Wakioka, A. Sasaki, R. Kato, T. Shouda, A. Matsumoto, K. Miyoshi, M. Tsuneoka, S. Komiya, R. Baron, A. Yoshimura, Spred is a Sprouty-related suppressor of Ras signalling, Nature 412 (2001) 647-651.

[18] N.J. Baeg, H.C.J. Bodenheimer, K. Burchard, Long-term sequellae of

acetaminophen-associated fulminant hepatic failure: relevance of early histology, Am. J. Gastroenterol. 83 (1988) 569-571.

[19] Y. Ishida, T. Kondo, T. Ohshima, H. Fujiwara, Y. Iwakura, N. Mukaida, A pivotal involvement of IFN-gamma in the pathogenesis of acetaminophen-induced acute liver injury, Faseb J. 16 (2002) 1227-1236.

[20] Z.X. Liu, S. Govindarajan, N. Kaplowitz, Innate immune system plays a critical role in determining the progression and severity of acetaminophen hepatotoxicity, Gastroenterology 127 (2004) 1760-1774.

[21] J.R. Groom, A.D. Luster, CXCR3 ligands: redundant, collaborative and antagonistic functions, Immunol. Cell Biol. 89 (2011) 207-215.

[22] M. Bilzer, F. Roggel, A.L. Gerbes, Role of Kupffer cells in host defense and liver disease, Liver Int. 26 (2006) 1175-1186.

[23] D. Datta, J.A. Flaxenburg, S. Laxmanan, C. Geehan, M. Grimm, A.M. Waaga-Gasser, D.M. Briscoe, S. Pal, Ras-induced modulation of CXCL10 and its receptor splice variant CXCR3-B in MDA-MB-435 and MCF-7 cells: relevance for the development of human breast cancer, Cancer Res. 66 (2006) 9509-9518.

[24] G. Beldi, Y. Wu, Y. Banz, M. Nowak, L. Miller, K. Enjyoji, A. Haschemi, G.G. Yegutkin, D. Candinas, M. Exley, S.C. Robson, Natural killer T cell dysfunction in CD39-null mice protects against concanavalin A-induced hepatitis, Hepatology 48 (2008) 841-852.

[25] J.A. Hobbs, S. Cho, T.J. Roberts, V. Sriram, J. Zhang, M. Xu, R.R. Brutkiewicz, Selective loss of natural killer T cells by apoptosis following infection with lymphocytic choriomeningitis virus, J. Virol. 75 (2001) 10746-10754.

[26] B. Gao, S. Radaeva, O. Park, Liver natural killer and natural killer T cells: immunobiology and emerging roles in liver diseases, J. Leukoc. Biol. 86 (2009) 513-528.

[27] Y. Maekawa, S. Tsukumo, H. Okada, K. Kishihara, K. Yasutomo, Breakdown of

peripheral T-cell tolerance by chronic interleukin-15 elevation, Transplantation 76 (2003) 415-420.

[28] U. Lee, K. Santa, S. Habu, T. Nishimura, Murine asialo GM1+CD8+ T cells as novel interleukin-12-responsive killer T cell precursors, Jpn. J. Cancer Res. 87 (1996) 429-432.

[29] E. Brillard, J.R. Pallandre, D. Chalmers, B. Ryffel, A. Radlovic, E. Seilles, P.S. Rohrlich, X. Pivot, P. Tiberghien, P. Saas, C. Borg, Natural killer cells prevent CD28-mediated Foxp3 transcription in CD4+CD25- T lymphocytes, Exp. Hematol. 35 (2007) 416-425.

[30] S. Roy, P.F. Barnes, A. Garg, S. Wu, D. Cosman, R. Vankayalapati, NK cells lyse T regulatory cells that expand in response to an intracellular pathogen, J. Immunol. 180 (2008) 1729-1736.

[31] M.J. Masson, L.D. Carpenter, M.L. Graf, L.R. Pohl, Pathogenic role of natural killer T and natural killer cells in acetaminophen-induced liver injury in mice is dependent on the presence of dimethyl sulfoxide, Hepatology 48 (2008) 889-897.

[32] P.D. Krueger, M.G. Lassen, H. Qiao, Y.S. Hahn, Regulation of NK cell repertoire and function in the liver, Crit. Rev. Immunol. 31 (2011) 43-52.

[33] H. Jaeschke, G.J. Gores, A.I. Cederbaum, J.A. Hinson, D. Pessayre, J.J. Lemasters, Mechanisms of hepatotoxicity, Toxicol. Sci. 65 (2002) 166-176.

[34] R.D. Goldin, I.D. Ratnayaka, C.S. Breach, I.N. Brown, S.N. Wickramasinghe, Role of macrophages in acetaminophen (paracetamol)-induced hepatotoxicity, J. Pathol. 179 (1996) 432-435.

[35] C. Ju, T.P. Reilly, M. Bourdi, M.F. Radonovich, J.N. Brady, J.W. George, L.R. Pohl, Protective role of Kupffer cells in acetaminophen-induced hepatic injury in mice, Chem. Res. Toxicol. 15 (2002) 1504-1513.

[36] M.P. Holt, L. Cheng, C. Ju, Identification and characterization of infiltrating macrophages in acetaminophen-induced liver injury, J. Leukoc. Biol. 84 (2008)

1410-1421.

[37] D.M. Dambach, L.M. Watson, K.R. Gray, S.K. Durham, D.L. Laskin, Role of CCR2 in macrophage migration into the liver during acetaminophen-induced hepatotoxicity in the mouse, Hepatology 35 (2002) 1093-1103.

[38] X. Ren, A. Kennedy, L.M. Colletti, CXC chemokine expression after stimulation with interferon-gamma in primary rat hepatocytes in culture, Shock 17 (2002) 513-520.

Figure legends

Figure 1　APAP-induced liver injury. WT and Spred-2 KO mice were i.p. injected with APAP (400 mg/kg). (A) Spred-2 expression in the liver after APAP challenge was measured in WT mice (4-6 mice, each point). Inset; Spred-2 expression was not detected in Spred-2 KO-liver (representative data). †$p<0.05$, vs. non-treated mice. (B) Serum ALT levels were measured after APAP challenge (6-12 mice, each point). †$p<0.05$, vs. WT mice. (C) The representative photographs of the liver sections after APAP challenge were shown. Arrowheads indicate injured area (original magnification × 200). (D) Injured area was measured using H&E sections by NIH image (6-12 mice, each point). †$p<0.05$, vs. WT mice.

Figure 2　Hepatocyte apoptosis in APAP-induced liver injury. WT and Spred-2 KO mice were i.p. injected with APAP (400 mg/kg). At 6 h after the injection, mice were killed. (A) Representative fluoromicroscopic photographs of liver sections with TUNEL staining were shown (original magnification × 200). (B) The numbers of TUNEL-positive hepatocytes/mm^2 were counted in WT-liver (12 mice) and Spred-2 KO-liver (15 mice). ‡$p<0.01$, vs. WT-liver. (C) Activities of caspase-3, -8 and -9 in WT-liver (10 mice) and Spred-2 KO-liver (12 mice). Dot lines were basal level of caspase activities from non-treated mice. †$p<0.05$ vs. WT mice. (D) The mRNA expressions of FasL and Fas in the WT-liver (10 mice) and Spred-2 KO-liver (12 mice) were analyzed by quantitative RT-PCR. The expression levels of each mRNA were normalized by β-actin. †$p<0.05$ vs. WT mice.

Figure 3　Analysis of hepatic lymphocytes after APAP Challenge. At 6 h after APAP (400 mg/kg) challenge, hepatic leukocytes were isolated from WT and Spred-2 KO mice (10-14 mice, each point), and stained with FITC- or PE-conjugated mAbs and

analyzed by flow cytometry. (A) Total leukocyte numbers in the liver were shown. (B) Cell numbers in the liver in each population were shown. The number of leukocyte populations in each liver was calculated by multiplying the respective percentages, as determined via flow cytometry, by total hepatic leukocyte counts. Dot lines were basal level of cell numbers of each population from non-treated mice. ‡$p<0.05$, †$p<0.01$ vs. WT controls.

Figure 4   Augmented cytokine response and MAPK activation in Spred-2 KO mice. At 6 h after APAP challenge (400 mg/kg), WT and Spred-2 KO mice (10 mice, each) were killed and the livers were harvested. (A) Serum levels of IFNγ, CXCL9 and CXCL10 were measured by ELISA. †$p<0.01$ vs. WT controls. (B) Hepatic mRNA expressions of CXCL9, CXCL10 and CXCR3 were quantitated by Taqman RT-PCR. The expression levels of each mRNA were normalized by GAPDH. ‡$p<0.05$ vs. WT controls. (C) Hepatic lymphocytes were stained with FITC- or PE-conjugated mAbs and analyzed by flow cytometry. ‡$p<0.05$, †$p<0.01$ vs. WT controls. (D) Livers were harvested at 6 h after APAP challenge and the extracts were immunoblotted with indicated antibodies. Shown are representative data from 2 mice each.

Figure 5   Kupffer cells as a source of CXCL9 and CXCL10. (A) WT and Spred-2 KO mice were i.p. injected with APAP (400 mg.kg). At 4 h after the injection, mice were killed and the livers were harvested (5 each). Kupffer cells were isolated from the liver and mRNA expressions of CXCL9 and CXCL10 were quantitated by Taqman RT-PCR. The expression levels of each mRNA were normalized by GAPDH. Shown are representative data from 2 independent experiments. †$p<0.01$, ¶$p<0.0001$ vs. WT controls. (B and C) Kupffer cells were isolated from non-treated WT and Spred-2 KO-liver (5 each) and stimulated with (B) APAP (10 μg/ml) and (C) IFNγ (10 ng/ml) for 4 h at 37°C, after which the mRNA expressions of CXCL9 and CXCL10 in the cells

were quantitated by Taqman RT-PCR. The expression levels of each mRNA were normalized by GAPDH. Shown are representative data from 2 independent experiments. ‡$p<0.05$, §$p<0.001$, ¶$p<0.0001$ vs. WT controls.

Figure 6 NK cells play a crucial role in the exacerbated liver injury in Spred-2 KO mice. Spred-2 KO mice were pretreated with rabbit anti-asialo GM1 (ASGM1) serum (10 mice) or control rabbit serum (10 mice) (20 μl/mouse, i.p.) 12 h prior to APAP challenge, and the mice were i.p. injected with APAP (400 mg/kg). At 12 h after APAP challenge, the mice were killed and the livers were resected. (A) Hepatic IFNγ mRNA expression was quantitated by Taqman RT-PCR. The expression levels of each mRNA were normalized by GAPDH. (B) Serum levels of ALT were measured. (C) Left: The representative photographs of the liver sections. Arrowheads indicate injured area (original magnification × 200). Right: Injured area was measured using H&E sections by NIH image. (D) Hepatic lymphocytes were stained with FITC- or PE-conjugated mAbs and analyzed by flow cytometry. (E) Hepatic lymphocytes were stained with FITC- or PE-conjugated mAbs and analyzed by flow cytometry. The number of IFNγ positive cells in each liver was calculated by multiplying the respective percentages, as determined via flow cytometry, by total hepatic leukocyte counts. ‡$p<0.05$, †$p<0.01$ vs. WT controls.

Figure 1

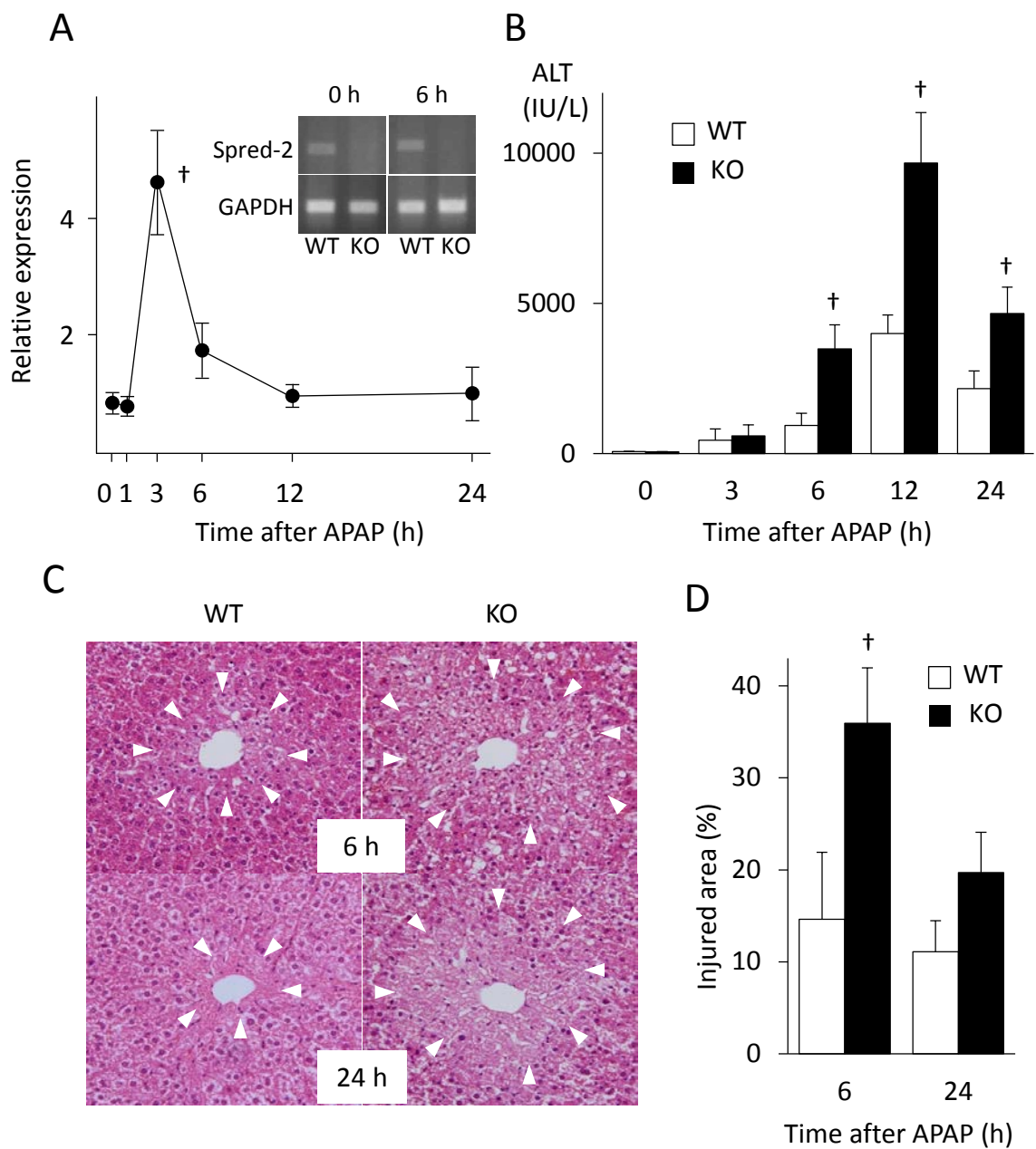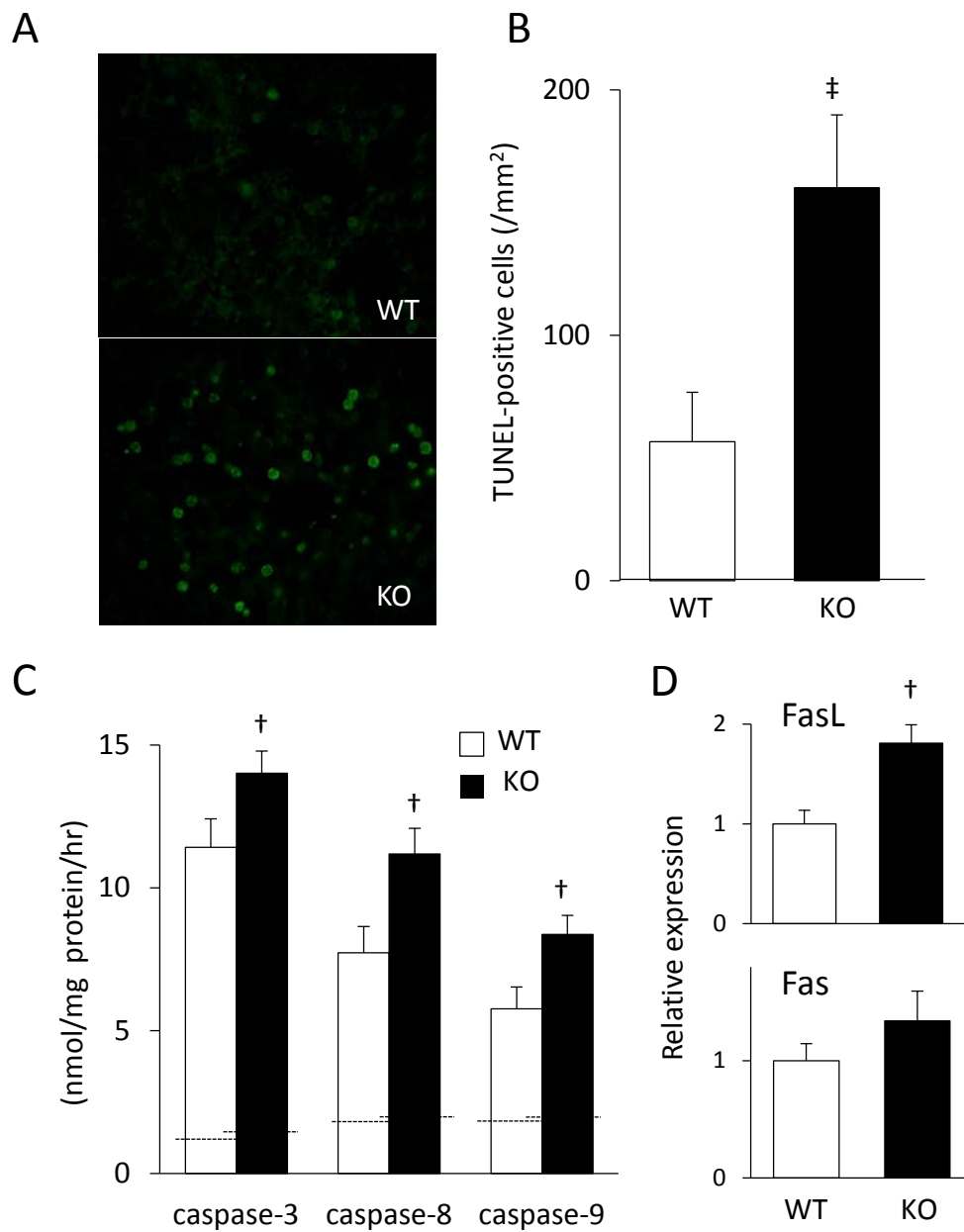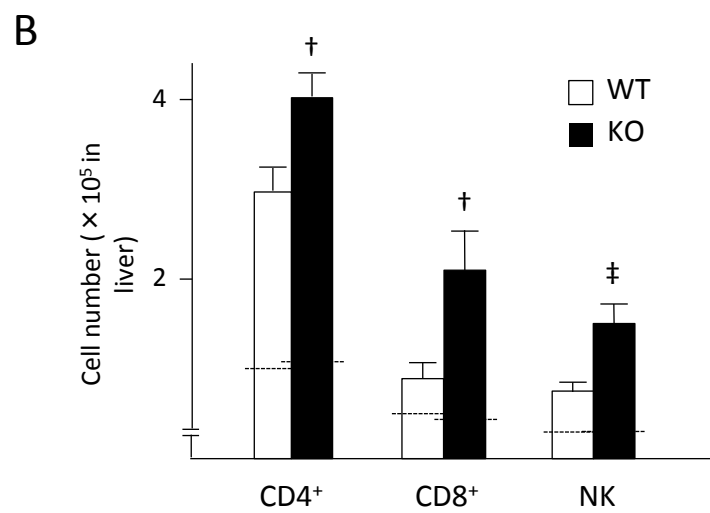Figure 2

Figure 3

A

Cell number ($\times 10^6$ in liver)

WT
KO

Time after APAP (h)

B

Cell number ($\times 10^5$ in liver)
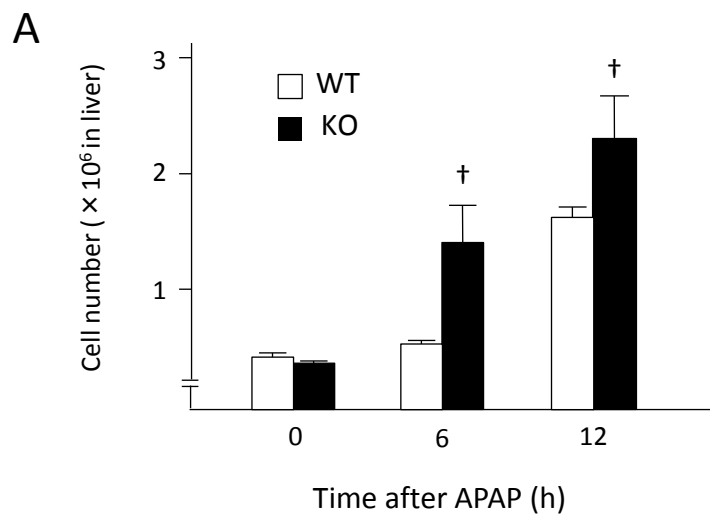
WT
KO

CD4$^+$ CD8$^+$ NK

Figure 4
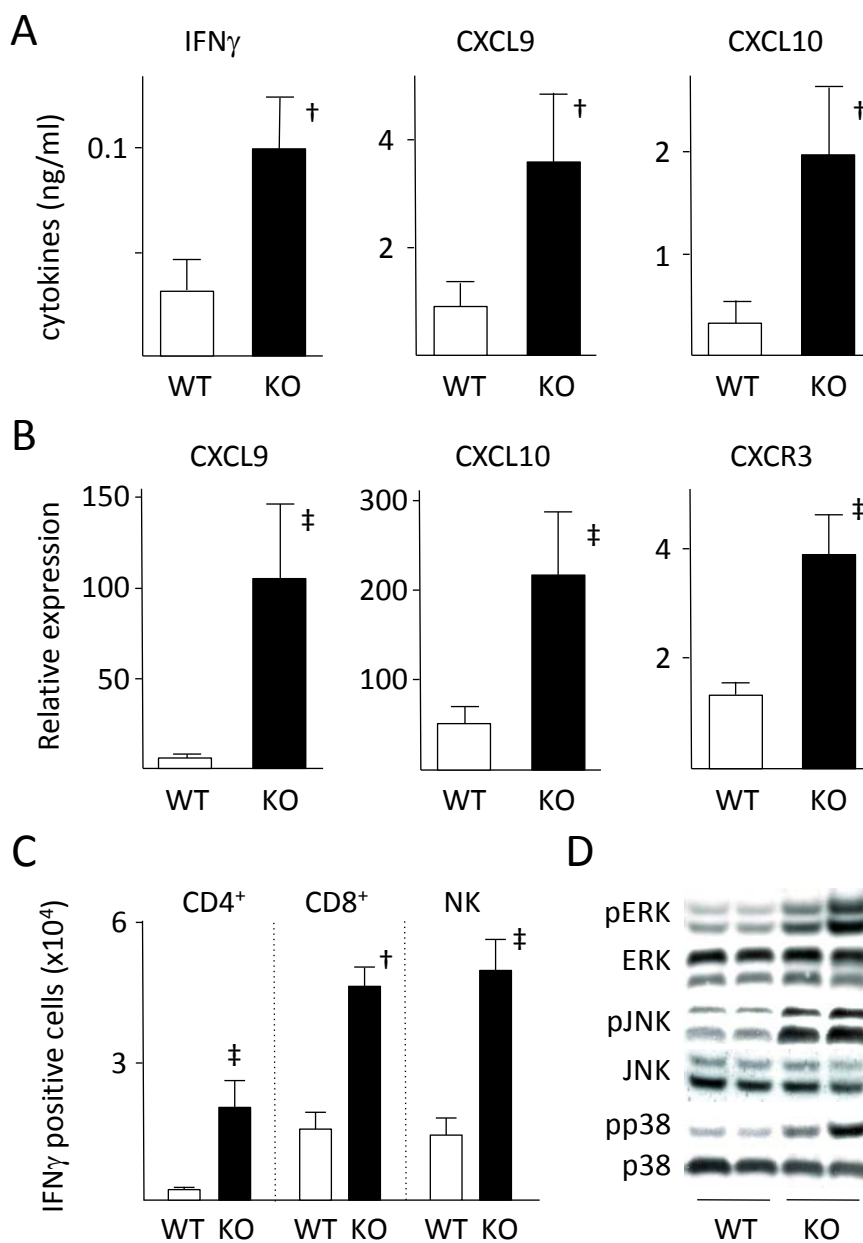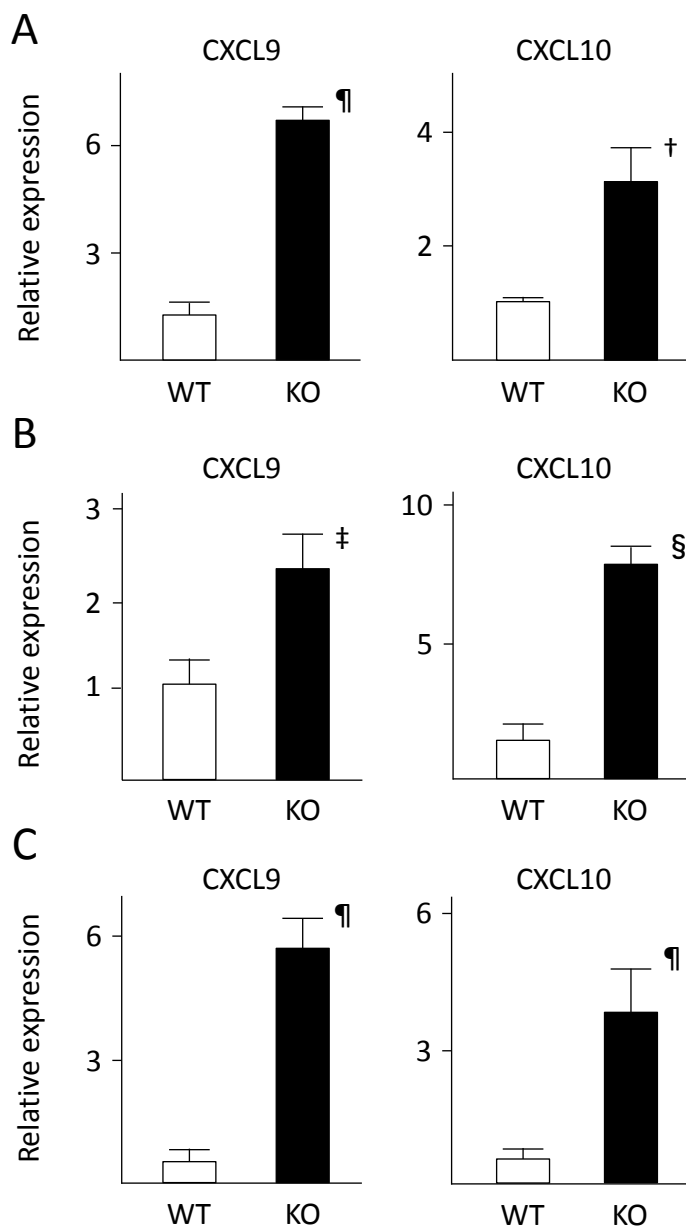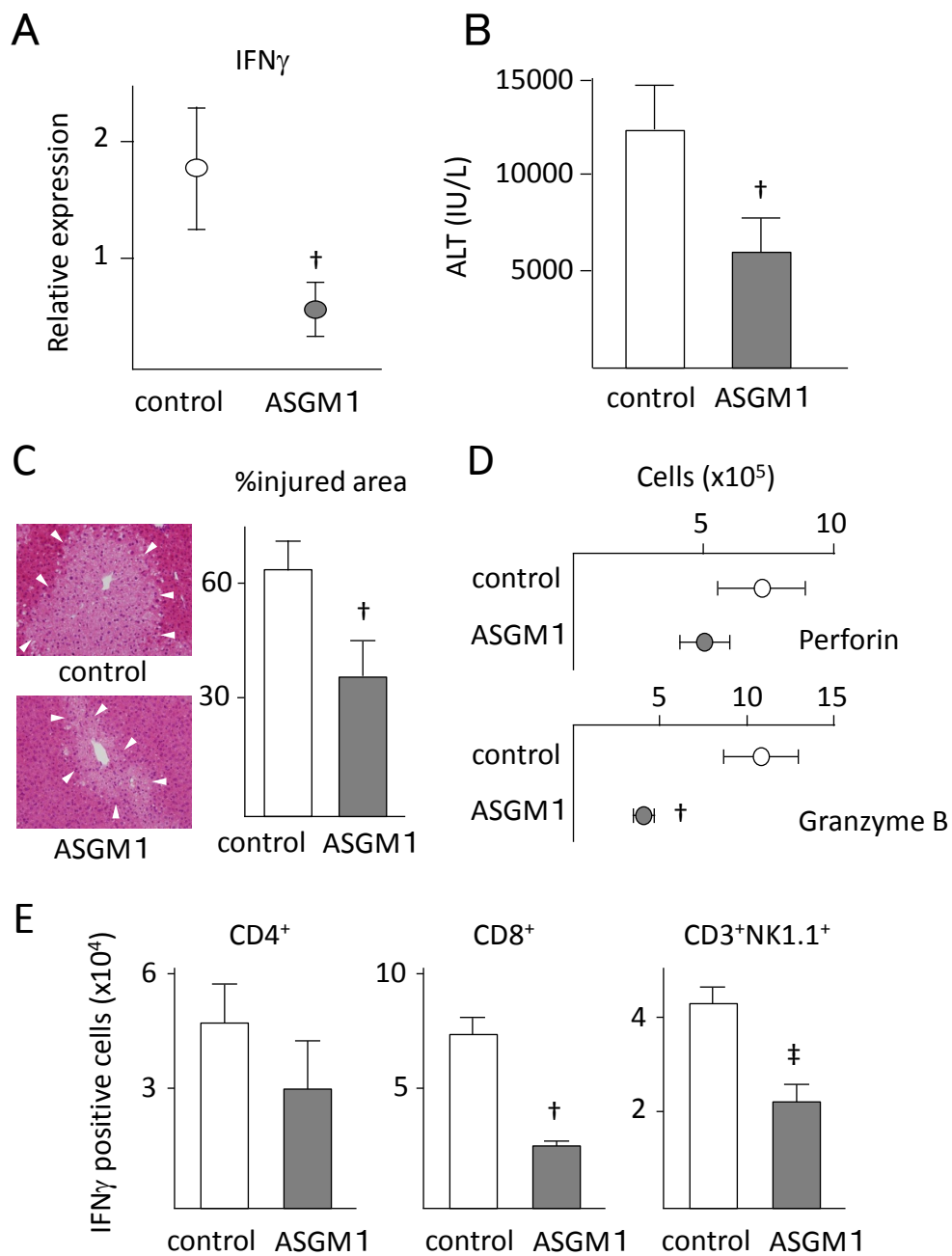
Figure 5

Figure 6

Table 1   The numbers of leukocyte populations in the liver after ASGM1 treatment

cell types	control ($\times 10^5$ cells)	ASGM1 ($\times 10^5$ cells)
CD3$^-$NK1.1$^+$	8.7 ± 1.4	1.1 ± 0.3 §
CD3$^+$NK1.1$^+$	28.6 ± 4.4	34.0 ± 2.8
CD4$^+$CD8$^-$	9.7 ± 2.0	5.2 ± 0.7 ‡
CD4$^-$CD8$^+$	11.2 ± 3.2	4.4 ± 0.6 ‡
CD4$^+$FoxP3$^+$	1.8 ± 0.3	4.0 ± 1.5
CD11b$^+$F4/80$^+$	6.6 ± 2.3	8.1 ± 2.3
CD11b$^+$Ly6G$^+$	28.9 ± 11.1	14.7 ± 3.0

Spred-2 KO mice were pretreated with rabbit anti-asialo GM1 serum (ASGM1: 10 mice) or control rabbit serum (10 mice) 12 h prior to APAP challenge. Hepatic lymphocytes were harvested at 6 h after APAP challenge and stained with FITC- or PE-conjugated mAbs and analyzed by flow cytometry. ‡$p<0.05$, §$p< 0.001$, vs. WT controls.